


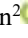






## Application of Finite Element Method to Analyze Fluid Dynamic and Stability Analysis Offshore Wind Turbine Power Foundation Model

Ngoc Thai Huynh<sup>1</sup>, Hoang Vinh Nguyen<sup>1</sup>, Minh Hung Vu<sup>2</sup>, Tien Dung Nguyen<sup>2</sup>, Trieu Khoa Nguyen<sup>3\*</sup>,  
Quoc Manh Nguyen<sup>4</sup>

<sup>1</sup> Faculty of Mechanical Engineering Technology, Ho Chi Minh City University of Industry and Trade, Ho Chi Minh City 700000, Vietnam

<sup>2</sup> Faculty of Fundamental Sciences, PetroVietnam University, Ba Ria 790000, Vietnam

<sup>3</sup> Faculty of Mechanical Engineering, Industrial University of Ho Chi Minh City, Ho Chi Minh City 700000, Vietnam

<sup>4</sup> Faculty of Mechanical Engineering, Hung Yen University of Technology and Education, Khoai Chau 160000, Vietnam

Corresponding Author Email: [nguyenkhoatrieu@juh.edu.vn](mailto:nguyenkhoatrieu@juh.edu.vn)

Copyright: ©2025 The authors. This article is published by IETA and is licensed under the CC BY 4.0 license (<http://creativecommons.org/licenses/by/4.0/>).

<https://doi.org/10.18280/ijht.430313>

### ABSTRACT

**Received:** 22 April 2025

**Revised:** 10 June 2025

**Accepted:** 18 June 2025

**Available online:** 30 June 2025

#### **Keywords:**

*offshore wind power foundation, hydrodynamics, aerodynamics, finite element method, ANSYS fluent*

Offshore wind energy is a promising solution for clean power generation but poses challenges in foundation design due to complex marine environments. This investigation applies the finite element method (FEM) to analyze the hydro-aerodynamic behavior of structures under the influence of wind and ocean waves. Models with varying brace bar diameters and thicknesses were created using Autodesk Inventor. Wind and wave loads were modeled by using fluid dynamic tool in ANSYS. The structural behavior under such loading conditions was measured by using the analysis static structural tool in ANSYS. The effects of wind velocity and ocean waves on the structural models with varying brace bar diameter and thickness, were measured. Results show that increasing flow velocity from 50 m/s to 60 m/s leads to a rise in impact pressure from 0.0096 MPa to 0.0157 MPa and deformation from 6.7263 mm to 6.9291 mm. Increasing the brace bar diameter and thickness dimensions from 400 mm × 20 mm to 600 mm × 40 mm reduced stress from 96.29 MPa to 80.14 MPa. With the results achieved, when designing the offshore wind turbine power foundation model, it is necessary to consider the recommended dimensions to ensure the structural stability during work.

## 1. INTRODUCTION

Offshore wind turbine is one of the structures or devices invented to collect wind and convert it into electricity and is a popular research topic in the world. Wind power base is one of the important parts used for fixing and installing under the sea. A combined CFD–FEA approach [1] was implemented to comprehensively simulate the response of a floating offshore wind turbine (FOWT) under wind and wave loading: CFD uses VOF, DFBI, and sliding mesh to capture the air–water flow and calculate the forces, while explicit nonlinear dynamic FEA evaluates the structural deformation, and the loading data from CFD are then fed into one-way FEA. On a NREL 5MW model with a mooring catenary, simulations under a variety of wind, wave, and wave direction conditions show that aero-hydrodynamic loading significantly affects the motion response (surge, heave, pitch) and deformation – providing reliable information for optimizing the FOWT structural design. A new dynamic [2] model has been developed for floating offshore wind turbines (FOWTs) that integrates mooring-anchor-soil interactions, challenging the traditional assumption of a fixed seabed anchor. Using the CEL method in Abaqus, the study represents complex anchor–chain–soil behavior through equivalent stiffness and damping, and fully

couples it with aerodynamic–hydrodynamic models in OpenFAST and Orcaflex. Results show that conventional models underestimate the platform’s peak horizontal motion and overestimate mooring line tension, while the new coupled model more accurately captures FOWT dynamic behavior by including the anchor foundation’s influence. The structural integrity of wind turbines [3] under wind loads using a two-pronged approach: first with a meticulously constructed 1/100 scale model in a wind tunnel, and second with advanced CFD simulations. Both methods accounted for the spacing between turbines. The tower design was evaluated under lateral, gravitational, and notable rotational blade loads, the latter analyzed in Abaqus by applying angular velocity to compute time-dependent support reactions via Newmark’s method. Equivalent static forces were derived, and results showed that maximum displacement aligns with the initial phase of rotor motion, offering valuable insights into turbine structural response under wind loading. The work applies high-resolution CFD–FEA coupling [4] to floating vertical-axis wind turbines (VAWTs) by creating a validated aero-hydro-moor-elastic model. Simulating a full-scale straight-bladed VAWT, it reveals that tower behavior is complex—showing mixed structural modes and combined wind-wave frequency effects—unlike blades or moorings,

which respond to a single environmental force. The study highlights the need for detailed coupled analysis to accurately capture amplified tower responses in offshore settings. A fully coupled aero-hydro-moor-elastic model [5] was applied for floating vertical-axis wind turbines (VAWTs) using CFD–FEA coupling. Validated against experimental data, the model simulates a full-scale straight-bladed VAWT under realistic environmental conditions. Results reveal that tower dynamics are complex, exhibiting combined 2-node and 3-node modes with wind- and wave-frequency effects. Unlike blades or floaters, the tower's response is amplified by simultaneous wind-wave interactions. The universal framework [6] for coupled dynamic analysis of floating wind farms with shared mooring systems has been developed and validated, incorporating hydrodynamic and structural coupling. This framework facilitates comprehensive simulations of dynamic behaviors under unsteady wind inflow, wave incidence, and mooring line dynamics, offering valuable insights for practical engineering applications. Additionally, the study investigates the dynamic responses following mooring line failures, highlighting risks of collision and progressive failure, thereby providing a methodology for assessing the reliability of floating wind farms with shared mooring systems. The integrated numerical model OlaFlow–ABAQUS [7] was utilized to analyze the dynamic behavior of a thin-walled steel monopile offshore wind turbine (OWT) and its seabed foundation under extreme wind and wave loads, simulating typhoon conditions. The results revealed significant dynamic interactions, including transient liquefaction zones in the seabed and approximately 0.4 m horizontal displacement at the tower top, leading to a  $0.51^\circ$  tilt of the OWT. This inclination may induce stress concentrations in mechanical components, potentially reducing the OWT's service life and affecting long-term performance. The novel wind-wave hybrid system combining floating offshore wind turbines (FOWTs) and wave energy converters (WECs) [8], were applied to enhance ocean renewable energy extraction. Utilizing the computational fluid dynamics (CFD) in OpenFOAM. The results demonstrated that the hybrid system significantly reduced platform motions and improved stability compared to standalone FOWTs, while also enhancing wave-shedding effects and maintaining acceptable mooring loads. The computational model for analyzing the dynamic interactions of floating offshore wind turbines (FOWTs) [9] was integrated dynamic fluid-body interaction with motion and catenary mooring solvers. The model employs overset mesh techniques to accurately simulate large-scale movements of the floating platform under wind and wave loads. Validation using the DeepCwind semi-submersible platform with the NREL 5-MW turbine demonstrates that the model effectively captures unsteady aerodynamic and hydrodynamic behaviors, offering insights into platform dynamics and mooring line tensions. The FssiCAS software platform and the open-source solver OlaFlow were applied [10] to analyze the dynamic characteristics and stability of a 1500 kW monopile offshore wind turbine (OWT) under typhoon conditions. The results indicate that the seabed foundation liquefies to a depth of 4–5 meters, leading to a horizontal displacement of approximately  $0.5^\circ$  in the tower cylinder, surpassing design limits. Wind loads contribute up to 50% to this lateral displacement and the maximum bending moment in the tower, highlighting the significant impact of wind forces on OWT stability. The study confirms that FssiCAS is a reliable tool for evaluating OWT dynamics and stability in complex marine environments. The

dynamic response of a 1500 kW monopile offshore wind turbine (OWT) [11] under typhoon conditions using the FssiCAS platform and OlaFlow solver. The findings revealed that extreme wind and wave loads can cause seabed liquefaction up to 5 meters deep, leading to a  $0.5^\circ$  tilt in the turbine tower. Wind loads contributed up to 50% to this lateral displacement, highlighting the significant impact of wind forces on OWT stability. The study also demonstrated the applicability of FssiCAS for evaluating OWT dynamics in complex marine environments. The offshore wind turbine jacket foundations [12] were enhanced by applying topology optimization to reduce weight and enhance fatigue life. Using advanced computational methods and time-domain fatigue simulations on an OC4 jacket model, the study achieved a 35.2% mass reduction and a 37.2% increase in fatigue life compared to traditional designs. The optimized designs comply with international standards, offering a practical framework for cost-effective and durable offshore wind turbine foundations. The towing of large offshore wind turbine jacket foundations with triple suction buckets [13] conducted focusing on the use of air cushions for buoyancy during wet towing. Numerical analyses in both frequency and time domains accurately predict natural periods, towing forces, body motions, and air pressures, showing good agreement with experimental data. Results highlight that towing forces and speeds are particularly significant at the start of transit, providing useful insights for efficient transportation of these foundations. The surrogate-model-based optimization for offshore wind jacket foundations [14] utilized parameter sensitivity to reduce variables and genetic algorithms to optimize lightweight designs across varying water depths. Validated through dynamic analysis, buckling strength, and fatigue assessments, the method achieved up to 98.6% faster computation,  $\sim 35\%$  mass reduction, and  $\sim 37\%$  improved fatigue life. An enhanced Support Vector Regression model integrating intelligent optimization [15] for more accurate approximation of fatigue damage in offshore wind turbine support structures under hybrid (random & systematic) uncertainty. The optimized SVR achieves 31.2% lower MAE, and including both uncertainty types raises predicted failure probability by 0.64%, offering a more accurate and conservative fatigue reliability evaluation. Rising sea levels demand stronger wind turbine foundations [16], shifting from monopiles to piled jackets. This study enhances pile-soil interaction modeling by incorporating cyclic effects using a bounding surface plasticity-based t-z model within OpenFAST. Results from the NREL 5 MW turbine show that neglecting stiffness loss and deformation buildup can misrepresent system behavior, while the improved model better captures load transfer and structural response. Offshore wind turbine foundations mainly suffer fatigue damage from long-term ocean loads [17]. This study proposes an improved nonlinear fatigue model to better estimate short- and long-term fatigue in monopile foundations. This investigation compared the seismic performance of three offshore wind turbine foundations-monopile, pile jacket, and suction bucket-using Abaqus simulations [18]. Wind and earthquake loads were applied to assess dynamic response and fragility. Results show monopile-supported turbines have the highest top displacement, while pile jacket foundations experience the highest tower stress. The findings aid in seismic design of offshore wind turbines. The investigation simulated the hydrodynamics of a fish cage integrated with a monopile offshore wind turbine [19] using a porous media model and

validated CFD methods. Results show that higher net solidity reduces flow velocity inside and behind the cage, while greater cage draught increases side velocities downstream. Findings support the design of integrated offshore wind–aquaculture systems. The multi-bucket foundation floating platform (MBFFP) for transporting and installing multiple offshore wind turbine units [20] efficiently was investigated. Numerical simulations assess its stability, hydrodynamics, and structural reliability. Results show the platform maintains safe motion and stress levels under typical sea conditions, demonstrating its feasibility and potential to reduce offshore wind farm installation costs. The two-stage finite element method [21] to assess offshore wind turbine foundations under earthquake-induced soil liquefaction. Results show that liquefaction reduces seismic forces but increases settlement risk, especially with deeper soil stiffness loss. For deep pile designs, foundation settlement not steel structure strength was the key concern.

The novel in this investigation such as:

The current research of this thesis will also apply Ansys for simulation, such as: preparing the model with Design Modeler, then meshing the Mesh part, then simulating the fluid with Fluent, and finally simulating the deformation and stress with Static Structure. In addition, the model design will be performed by Inventor. The remaining step will be to conduct simulation and collect output data in Ansys. Unlike previous studies, using software such as ANSYS to analyze the two environments, air and water, acting on the base model will simulate visually and objectively.

- From the initial parameters, select two important parameter levels for design, such as diameter and thickness parameters.
- Select the necessary design parameter levels and conduct numerical experiments using Minitab software to optimize the experiments.
- Use Inventor to design 3 models and build a simulation environment.
- Apply the finite element method (FEM) to analyze the pressure, stress, and deformation factors of the foundation structure under the impact of fluid flow in a 50 m deep sea area.
- The study provides deeper knowledge of optimization algorithms in engineering design and mechanical structures.
- Combine theoretical knowledge learned at school and updated information from research documents to complete the design model.
- The study will serve as a foundation for expanding knowledge and developing practical applications in offshore wind power base design.

Supporting the implementation of offshore wind power and oil and gas projects domestically and internationally, meeting the demand for clean energy and reducing greenhouse gas emissions.

The offshore wind turbine power pedestal model is designed in the form of a tower-shaped space structure, with a quadrilateral pyramid shape that gradually rises vertically. The structure consists of four main columns located at four corners, connected together through a system of cross-bracing and horizontal bars, forming a sustainable space truss system. The bracing bars are arranged in a symmetrical X shape, ensuring good load-bearing capacity in both horizontal and vertical directions. The entire structure is simulated by truss elements, which bear the main load of axial force.

## 2. DESIGN OFFSHORE WIND TURBINE POWER PEDESTAL MODEL

The offshore wind turbine power pedestal type is designed as a spatial truss tower with a quadrilateral base that tapers toward the top. The four main vertical columns are positioned at each corner and are connected by a system of horizontal and diagonal bracing sections. Both horizontal and vertical load resistance are enhanced by the bracing bars' symmetrical X-shaped configuration. This design ensures structural stability under dynamic maritime conditions, including wind and wave forces. Truss components are used to model the structure in order to accurately depict the behavior of axial forces. The model's overall layout and structural underpinnings were depicted in Figure 1.

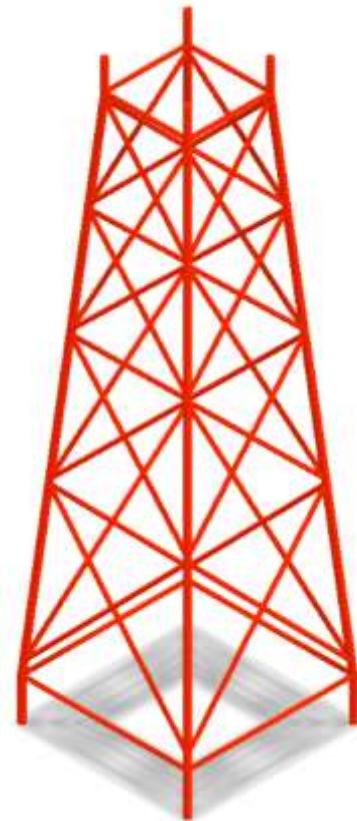


Figure 1. Wind power pedestal model designed by inventor

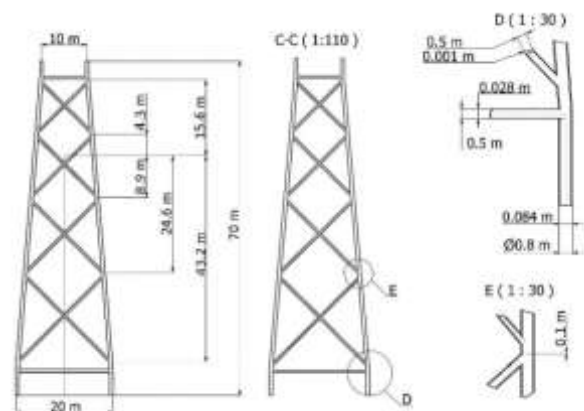


Figure 2. Projection of wind power pedestal model

Figure 2 illustrates the projected view of the offshore wind turbine pedestal model, providing a clearer representation of its geometric configuration and structural layout. This view highlights the symmetrical distribution of the diagonal and horizontal bracing elements, which play a crucial role in enhancing the structural stiffness and load-bearing capacity. The projection also emphasizes the tapering shape of the tower, which helps to minimize aerodynamic drag and improve overall stability under high wind and wave conditions.

### 3. FINITE ELEMENT ANALYSIS

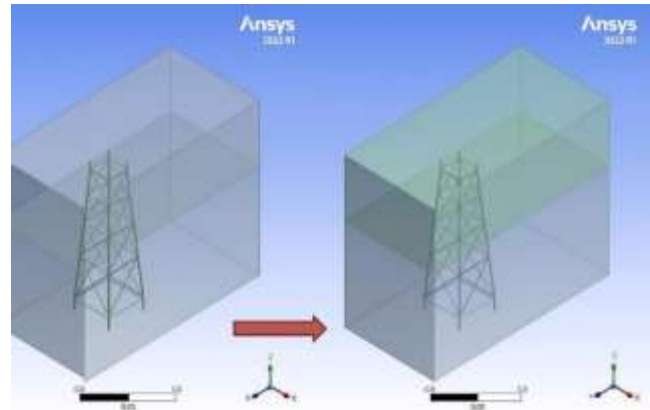
#### 3.1 Hydrodynamic and aerodynamic analysis

To simulate the relationship between the wind turbine structure and the environment, Boolean operations were used to create the computational domains for both air and water. The parameters and details of these procedures, including the subtract operation that generates flow regions around the model shape, are compiled in Table 1.

The fluid flow channels and structural boundaries were clearly distinguished in Figure 3, which depicted the fluid domain after Boolean subtraction. This was the computational domain that results. This phase was essential for accurate meshing and boundary condition setup during the simulation process.

**Table 1.** Using Boolean command to create obstacles in the environment

Details of Boolean1	
Boolean	Boolean1
Operation	Subtract
Target Bodies	2 Bodies
Tool Bodies	1 Body
Tool Bodies?	No



**Figure 3.** Domain generation results

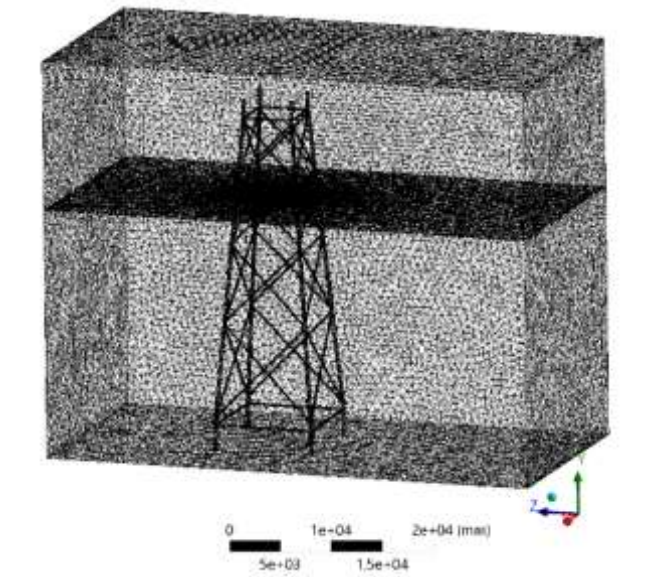
The following settings were shown in Table 2: Element mesh size: 400 mm and also set the defeature size parameter to 20 mm. The resulting mesh, shown in Figure 4, demonstrated a structured grid with consistent element distribution across the model surface, ensuring adequate resolution for fluid–structure interaction analysis in the simulation environment.

The selection of parameters to be included in the problem was essentially assigning conditions and attributes to solve the problem. The parameters included will determine the accuracy and optimization of the simulation.

Environmental parameters at the base installation location.

- Flow velocity: 3.09 m/s;
- Average wind velocity: 50 m/s;
- Water and air will follow the software;
- Ambient temperature used for the problem: 288.16 K equivalent to 15°C.

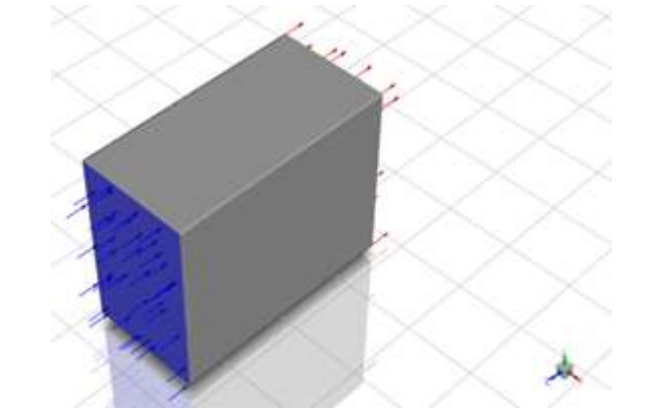
Figure 5 and Table 3 depicted the flow in the experimental domain through the offshore wind turbine foundation model.



**Figure 4.** Meshing result of model

**Table 2.** Parameters to set for creating mesh

Display	
Display style	Use Geometry setting
Defaults	
Physics preference	Mechanical
Element order	Program Controlled
Element size	400.0 mm
Sizing	
Use adaptive sizing	Yes
Resolution	Default (2)
Mesh defeaturing	Yes
Defeature size	20 mm
Transition	Fast
Span angle center	Coarse
Initial size seed	Assembly
Bounding box diagonal	68739 mm
Average surface area	37295000 mm <sup>2</sup>
Minimum edge length	0.03



**Figure 5.** Inlet & outlet in fluent



**Table 3.** Settings in fluent

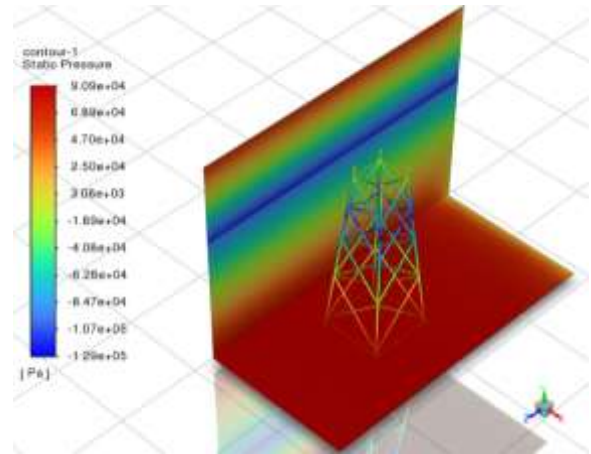
Category	Setting/Value
Seawater density (kg/m <sup>3</sup> )	1020
Solver	pressure based
Velocity formulation	absolute
Time	steady
Y gravity (m/s <sup>2</sup> )	-9.81
Models	
Viscous	Laminar
Air	
Density (Kg/m <sup>3</sup> )	1.225
Viscosity Kg/m s	1.7894e-05
Water-liquid	
Density (Kg/m <sup>3</sup> )	998.2
Viscosity Kg/m s	0.001003
Boundary conditions	
Inlet air (m/s)	39
Inlet water (m/s)	3.09
Outlet	
Prevent reverse flow	Yes
Velocity specification method	magnitude, normal to the boundary
Reference frame	absolute
Solution methods	
Pressure-velocity coupling	Yes
Scheme	coupled
Spatial discretization	
Gradient	Least Squares Cell-based
Pressure	Second-order
Momentum	Second-order Upwind
Pseudo transient	yes
Pressure	0.5
Momentum	0.5
Density	1
Body forces	1
Number of iterations	100

## 4. RESULTS AND DISCUSSIONS

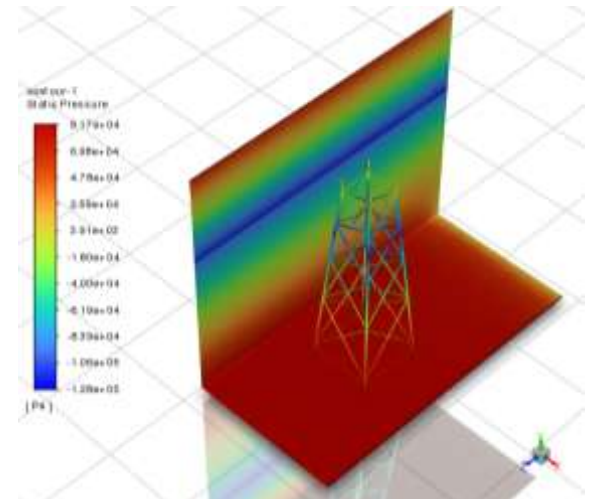
### 4.1 Fluid dynamic analysis

When changing the dimension of the object model in the Fluent flow simulation environment, the pressure distribution around the model changed significantly as presented in Figure 6. In models with a compact structure or a larger flow barrier area, the maximum pressure value at the surface directly facing the flow tends to increased, due to more resistance to the air flow, creating a greater impact force on the structure. At the same time, a more obvious low pressure area appears behind the model, showing the phenomenon of flow separation and creating air bubbles. The pressure difference between the front and back of the model also increases with the change in size, directly affecting the stress acting on the structure. In addition, changes in the shape of the model also lead to changes in the boundary of the pressure influence area, causing the force-bearing area to change accordingly. The more closed or complex the model is, the more uneven the pressure distribution is, requiring a more careful calculation of the stress analysis process. These results demonstrate the importance of selecting the appropriate size and shape when designing structures operating in flowing environments such as drilling platforms, transmission towers, or offshore structures. In this study, the design hydrostatic pressure referenced from the article "Structural Design of a Floating Foundation for Offshore Wind Turbine in Red Sea" is approximately 227000 Pa (corresponding to a water depth of

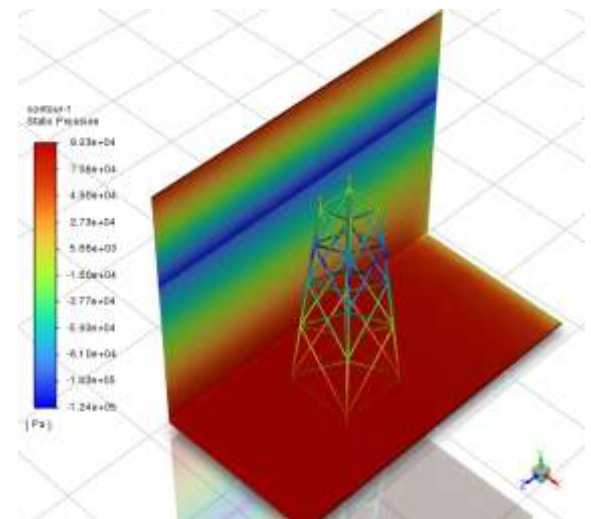
22.6 m). The simulation results from Fluent show that the pressure value ranges from 90230 Pa to 91700 Pa, which is approximately 60% lower than the design value. This may be due to differences in water depth, boundary conditions, or pressure measurement locations in the model. However, the results from Fluent have good stability with a small error of less than 2% between models.



a) Diameter and thickness of the brace bar: 600 mm and 40 mm

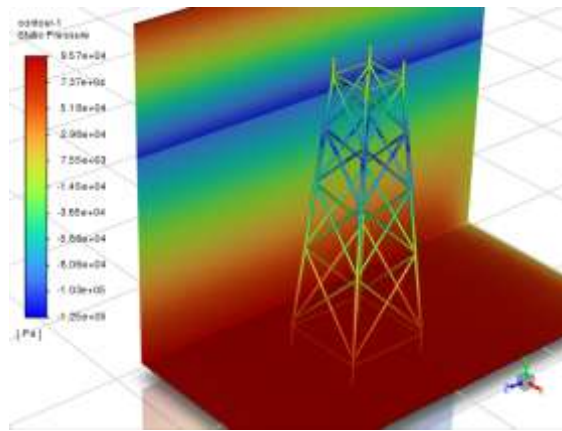


b) Diameter and thickness of the brace bar: 500 mm and 30 mm

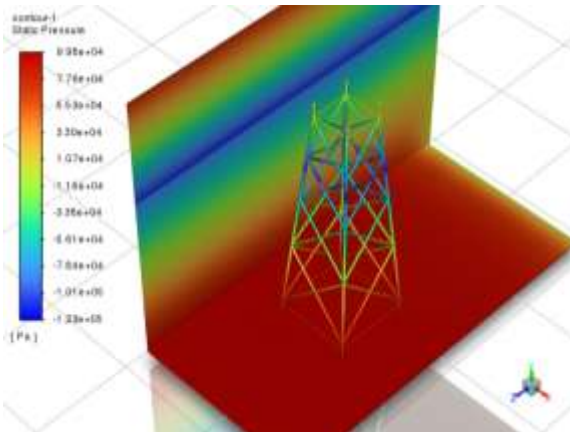


c) Diameter and thickness of the brace bar: 400 mm and 20 mm

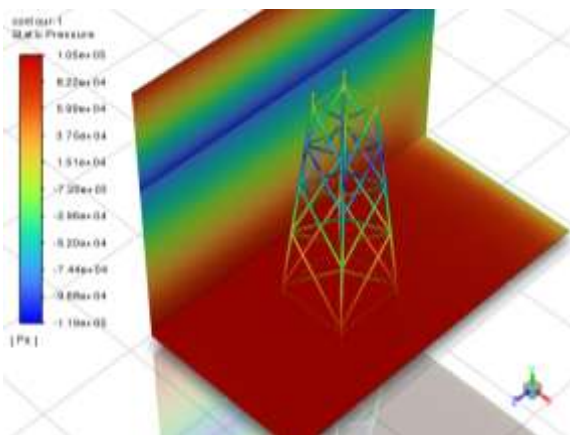
**Figure 6.** Hydro-aerodynamic analysis results



a)  $V_{\text{air}}=50 \text{ m/s}$ – $V_{\text{water}}=3.39 \text{ m/s}$



b)  $V_{\text{air}}=55 \text{ m/s}$ – $V_{\text{water}}=3.69 \text{ m/s}$



c)  $V_{\text{air}}=60 \text{ m/s}$ – $V_{\text{water}}=3.69 \text{ m/s}$

**Figure 7.** Hydro-aerodynamic analysis results with variable inlet speed

The maximum pressure level is about 0.0096 MPa, mainly concentrated on the front of the tower in the direction of the air flow. The structural deformation is still small and within the safe limit (Figure 7(a)).

The pressure value increases to about 0.0107 MPa, the pressure distribution is clearer with larger positive and negative pressure areas, reflecting the development of flow separation phenomenon behind the structure. The deformation increases slightly, especially at the base of the tower (Figure 7(b)).

The pressure reaches a maximum value of up to 0.0157 MPa, the highest level in all three cases. The difference between positive and negative pressure clearly shows the strong aerodynamic effect, significantly increasing the overall

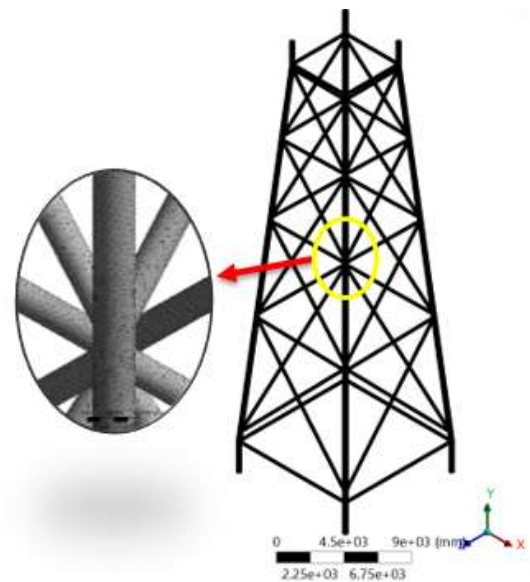
deformation of the structure, especially at the diagonal bars and the base where the load is concentrated (Figure 7(c)).

When increasing the flow velocity of fluid (gas and liquid) from 50 m/s to 55 m/s, the pressure acting on the model changes from 0.0096 MPa to 0.0157 MPa. and at a velocity of 60 m/s, the maximum pressure reaches about 0.0157 MPa.

The pressure acting on the wind turbine base was concentrated on the lower braces. This proved that the lower braces bear more pressure. With this result, it is recommended to increase the diameter of the lower braces to ensure the stable operation of the wind turbine base model.

## 4.2 The offshore wind power pedestal model durability analysis

The material chosen for analysis is steel. The mesh model in Figure 8 is created for the tower truss structure with a total of 1091309 nodes and 547149 elements. The element setup uses “Program Controlled” mode with a default element size of 150 mm, which shows that this is a fairly coarse mesh. The mesh generation method applies “Adaptive Sizing” with a resolution of “Default (2)”, which helps the software automatically refine the mesh density based on the complexity of the geometry. The “Mesh Defeaturing” property is enabled with a small detail filter size of 30 mm to remove small geometric details that do not greatly affect the analysis results. The “Fast” transition mode allows the software to quickly change the mesh density between different regions, suitable for models with uniform structures or not requiring too high local smoothness. Setting the “Span Angle Center” value to “Coarse” also helps reduce the number of elements and speed up the calculation.



**Figure 8.** Finite element model

The boundary conditions and loads applied to the model are set in Figure 9 as following:

- A (Fixed Support): The bases of the structure are completely fixed, not allowing for displacement or rotation, reflecting the connection conditions with the actual foundation.
- B (Pressure): The load applied to the model is the pressure obtained by the hydro-aerodynamic analysis.
- C (Standard Gravity): The gravitational acceleration of 9806.6 mm/s<sup>2</sup> is applied to the entire structure to consider the impact of the self-mass of the structural members.



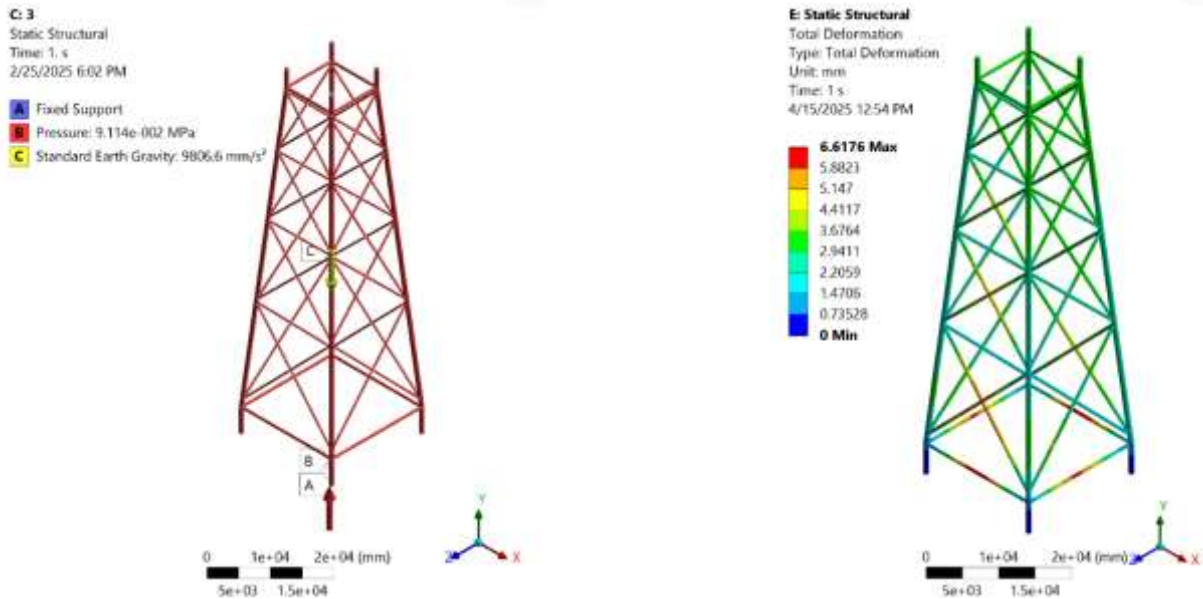
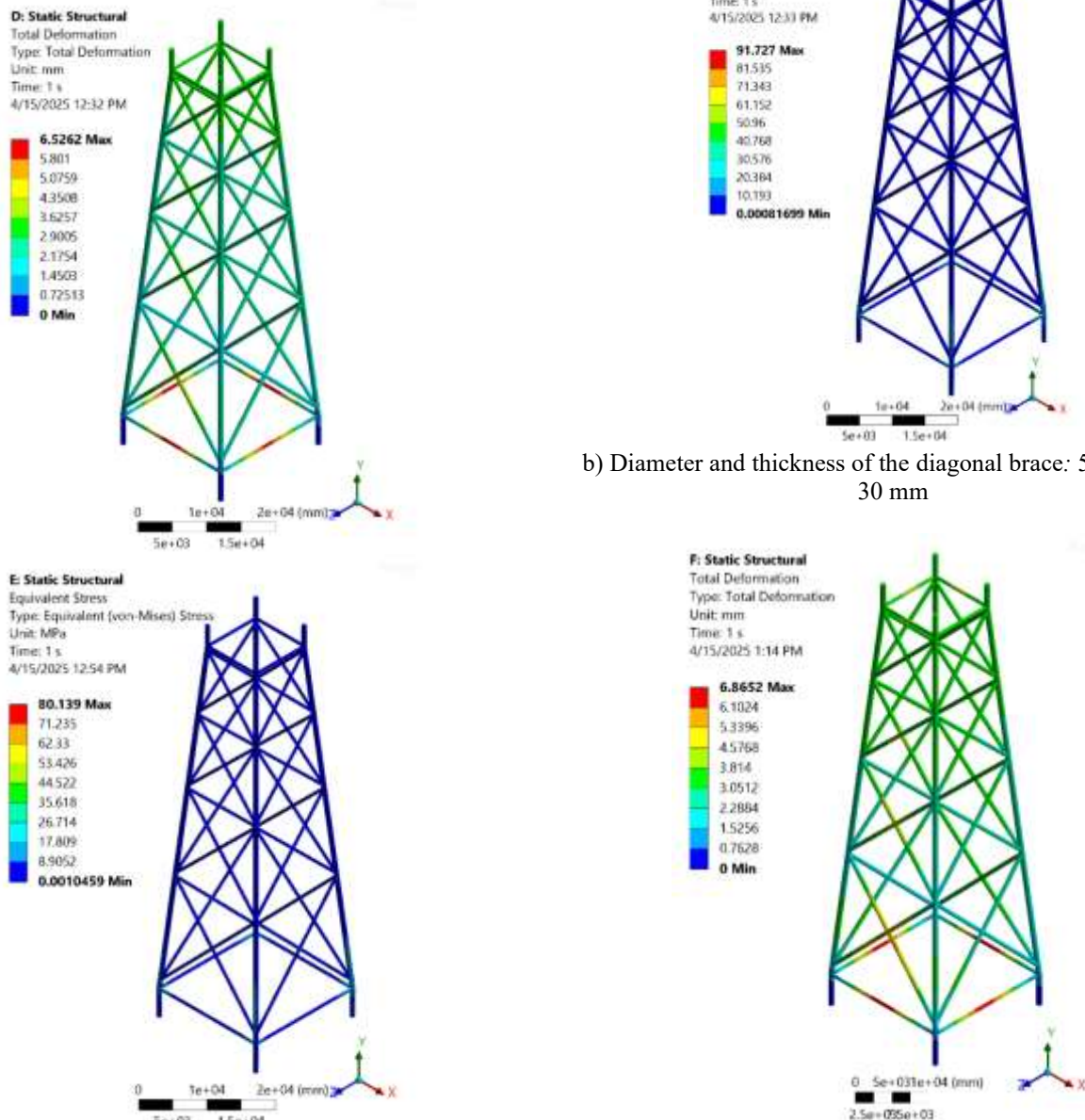
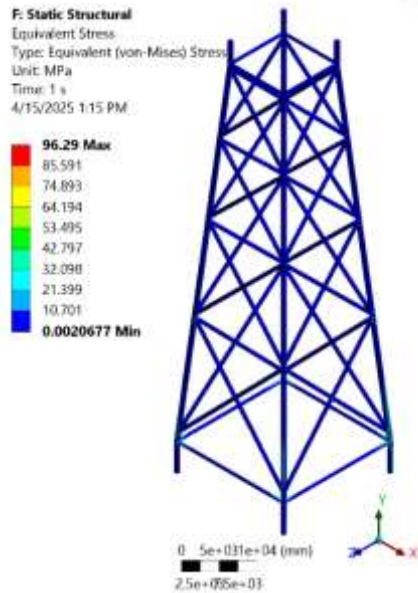


Figure 9. Set up loads and boundary conditions



b) Diameter and thickness of the diagonal brace: 500 mm and 30 mm

a) Diameter and thickness of the diagonal brace: 600 mm and 40 mm



c) Diameter and thickness of the diagonal brace: 400 mm and 20 mm

**Figure 10.** Strength analysis results with varying the brace bar diameter and thickness

The full and reasonable setting of the above conditions helps the model to more accurately reflect the actual mechanical behavior of the tower during the analysis.

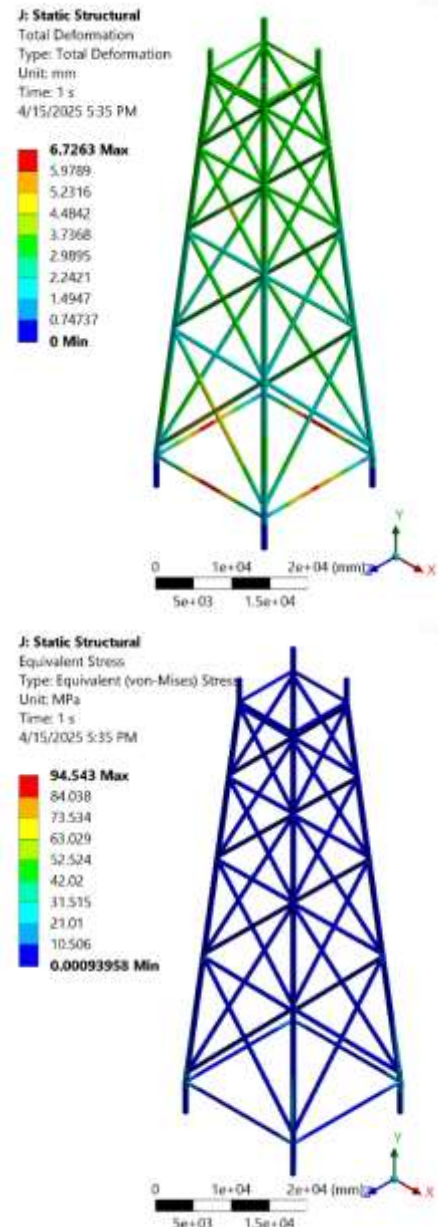
The three analyzed tower models have the same height and overall structure but differ in the size and thickness of the tie bars. When comparing the models, we can see that the deformation and stress trends are clearly different according to the size of the member. Figure 10(a) shows that the overall deformation is the smallest among the three models with a maximum value of about 5,622 mm, the equivalent stress is distributed quite evenly and low, reaching a maximum value of 14,509 MPa, proving that the model has good stiffness and high load-bearing capacity. Figure 2 shows that the overall deformation increases slightly with a maximum value of about 6,897 mm, the stress is slightly larger than Figure 10(b), reaching about 17,452 MPa, the structure still maintains stability but shows signs of poorer load-bearing capacity. Figure 10(c) shows that the deformation increased significantly, reaching a maximum of 6,952 mm, the equivalent stress reached 20,923 MPa, concentrated in the foot and diagonal bars, showing that the load-bearing capacity has clearly decreased. Overall, as the tie bar size and thickness decrease, the structural stiffness decreases, resulting in increased deformation and higher internal stress; Figure 10(a) model has the best bearing capacity, while Figure 10(c) is suitable for light loading conditions.

The three models in Figure 11 indicated that the effects of different air and water flow velocities on the tower structure. Figure 11(a) with air velocity of 55 m/s and water velocity of 3.39 m/s the overall deformation reaches about 4.7265 mm, the maximum stress is 84.534 MPa. When the velocity increased to 60 m/s and 3.69 m/s in Figure 11(b), the deformation increases to 6.0002 mm, the stress decreases to 76.989 MPa, showing the redistribution of the load when the fluid has a stronger impact. In Figure 11(c), with air velocity of 65 m/s and water velocity of 3.99 m/s, the deformation reaches the highest value of 6.9292 mm and the stress increases again to 98.007 MPa, concentrated in the diagonal bars and base. Thus, as the fluid flow velocity increases, the

structure tends to deform more and the stress fluctuates according to the change in flow conditions, reflecting the complex impact of hydro-aerodynamics on the structure. The greatest deformations and stresses are concentrated on the braces at the bottom of the wind turbine base. The problem made the damage of the offshore wind power foundation model focus on the braces below. Therefore, when designing, the diameter and thickness of the braces can be increased to ensure the stable operation of the offshore wind power foundation model.

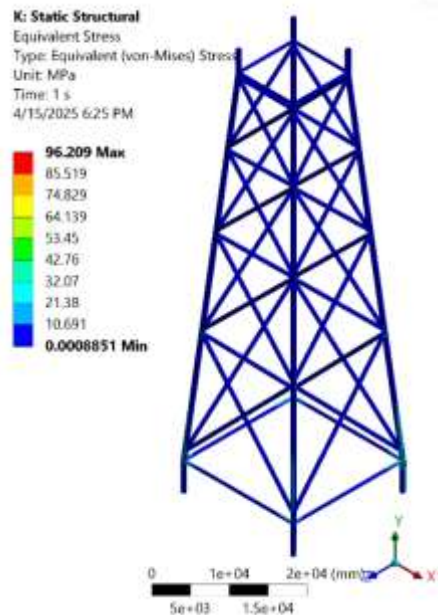
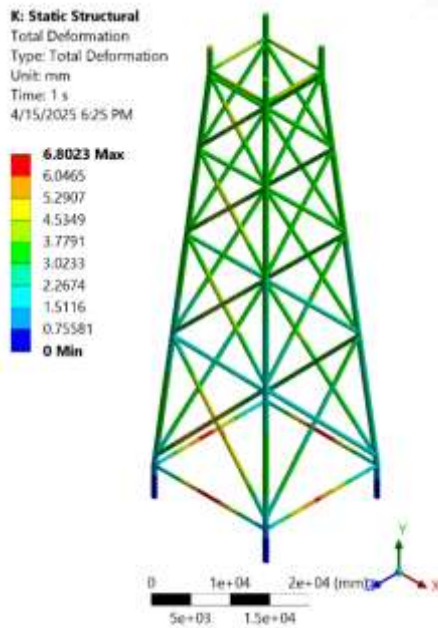
**Table 4.** Compare the results achieved with published works

Works	Pressure (MPa)	Displacement (mm)	Stress (MPa)
Current project	0.0157	9.929 mm	98.007
Reference [1]		73.04	561.3
Reference [3]		160	281.155
Reference [4]		5	200
Reference [7]	0.05		
Reference [10]	1	200	33.3
Reference [15]		2.447	85

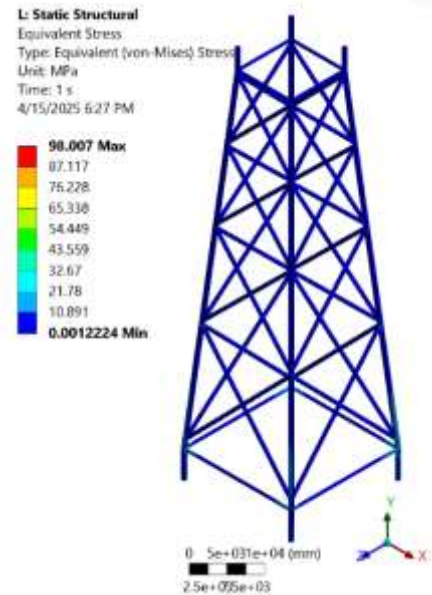
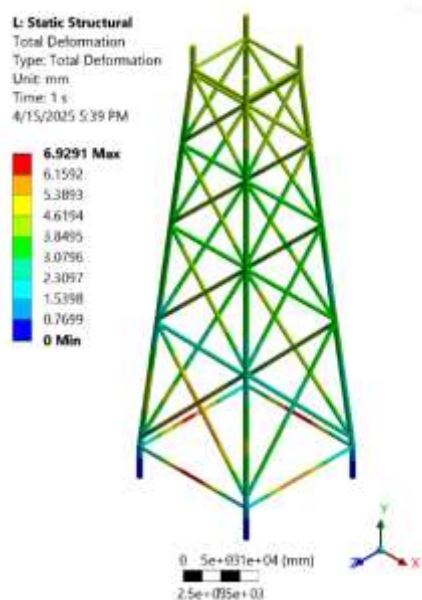


a) The impact pressure is 0.0960273 MPa





b) The impact pressure is 0.10075 MPa



c) The impact pressure is 0.105791 MPa

**Figure 11.** Durability analysis with pressure acting on the changing model

Comparison of current results with published works was shown in Table 4. This table indicated that most of the published works have wind power base models with larger deformations and stresses than the current works.

## 5. CONCLUSIONS

This study has leveraged finite element analysis (FEA), incorporating fluid–structure interaction via ANSYS, to scrutinize the hydro-aerodynamic response of offshore turbine foundation models under combined wind and wave forces. Parametric models with varying brace bar diameters and thicknesses were developed in Autodesk Inventor, and subjected to simulated loads reflecting extreme flow conditions.

The results reveal two key trends:

- Flow velocity dependence: As flow velocity increases from 50 m/s to 60 m/s, both pressure and deformation rise impact pressure climbs from 0.0096 MPa to 0.0157 MPa, while displacement increases slightly from 6.73 mm to 6.93 mm—demonstrating the nonlinear sensitivity of structural response to environmental loading.
- Brace bar geometry effect: Expanding brace bar dimensions from 400 mm × 20 mm to 600 mm × 40 mm leads to a pronounced reduction in stress levels—from approximately 96 MPa to 80 MP indicating that increased cross-sectional size boosts stiffness, enhancing resistance to deformation and load-induced stress.
- These findings align closely with established FEM-based design strategies for offshore foundations, which emphasize that larger structural dimensions and optimized bracing layout significantly improve dynamic performance and fatigue resistance under cyclic wind-wave loads.

## REFERENCES

- [1] Song, X.M., Bi, X.Q., Liu, W.Q., Guo, X.X. (2024).

- Numerical simulation of a floating offshore wind turbine in wind and waves based on a coupled CFD–FEA approach. *Journal of Marine Science and Engineering*, 12(8): 1385. <https://doi.org/10.3390/jmse12081385>
- [2] Qiao, D.S., Zhou, Y.C., Xu, B.B., Qin, J.M., Tang, G.Q., Lu, L., Ou, J.P. (2024). Dynamic response analysis of a fully coupled aerodynamic-hydrodynamic-mooring-anchor floating offshore wind turbine. *Ocean Engineering*, 312: 119085. <https://doi.org/10.1016/j.oceaneng.2024.119085>
- [3] Mansoubi, S., Sadeghi, H., Ma, Y., Mohebbi, R. (2024). An experimental and numerical investigation into the influence of wind effects on wind turbines with tubular towers. *Ocean Engineering*, 313: 119555. <https://doi.org/10.1016/j.oceaneng.2024.119555>
- [4] Luo, W.P., Liu, W.Q., Chen, S., Zou, Q.L., Song, X.M. (2024). Development and application of an FSI model for floating VAWT by coupling CFD and FEA. *Journal of Marine Science and Engineering*, 12(4): 683. <https://doi.org/10.3390/jmse12040683>
- [5] Haider, R., Li, X., Shi, W., Lin, Z.B., Xiao, Q., Zhao, H.S. (2024). Review of computational fluid dynamics in the design of floating offshore wind turbines. *Energies*, 17(17): 4269. <https://doi.org/10.3390/en17174269>
- [6] Zhang, Y.M., Liu, H.X. (2023). Coupled dynamic analysis on floating wind farms with shared mooring under complex conditions. *Ocean Engineering*, 267: 113323. <https://doi.org/10.1016/j.oceaneng.2022.113323>
- [7] Yu, D.W., Ye, J.H., Yin, C.Q. (2023). Dynamics of offshore wind turbine and its seabed foundation under combined wind-wave loading. *Ocean Engineering*, 286: 115624. <https://doi.org/10.1016/j.oceaneng.2023.115624>
- [8] Li, Y.N., Yan, S.Q., Shi, H.D., Ma, Q.W., Li, D.M., Cao, F.F. (2023). Hydrodynamic analysis of a novel multi-buoy wind-wave energy system. *Renewable Energy*, 219: 119477. <https://doi.org/10.1016/j.renene.2023.119477>
- [9] Huang, H.D., Liu, Q.S., Yue, M.N., Miao, W.P., Wang, P.L., Li, C. (2023). Fully coupled aero-hydrodynamic analysis of a biomimetic fractal semi-submersible floating offshore wind turbine under wind-wave excitation conditions. *Renewable Energy*, 203: 280-300. <https://doi.org/10.1016/j.renene.2022.12.060>
- [10] He, K.P., Ye, J.H. (2023). Dynamics of offshore wind turbine-seabed foundation under hydrodynamic and aerodynamic loads: A coupled numerical way. *Renewable Energy*, 202: 453-469. <https://doi.org/10.1016/j.renene.2022.11.029>
- [11] Marjanm, A., Huang, L.F., Hart, P. (2023). Structural fatigue assessment and optimisation of offshore wind turbine jacket foundations. *School of Water Energy and Environment of Cranfield University*, 1-172.
- [12] Arjomand, M.A., Bagheri, M., Mostafaei, Y. (2025). Performance enhancement of tuned liquid dampers in fixed offshore platforms: A coupled ANSYS Aqwa-transient structural approach. *Civil Engineering and Applied Solutions*, 1(1): 78-88. <https://doi.org/10.22080/ceas.2025.29085.1003>
- [13] Tan, L., Hu, C.H., Liu, Y.Y. (2023). Numerical simulations of towing a jacket foundation with triple buckets. *IOP Conference Series: Materials Science and Engineering*, 1288(1): 012033. <https://doi.org/10.1088/1757-899x/1288/1/012033>
- [14] Zheng, S.Y., Li, C., Xiao, Y.Q. (2023). Efficient optimization design method of jacket structures for offshore wind turbines. *Marine Structures*, 89: 103372. <https://doi.org/10.1016/j.marstruc.2023.103372>
- [15] Meng, D.B., Yang, S.Y., Yang, H.F., De Jesus, A.M.P., Correia, J., Zhu, S.P. (2024). Intelligent-inspired framework for fatigue reliability evaluation of offshore wind turbine support structures under hybrid uncertainty. *Ocean Engineering*, 307: 118213. <https://doi.org/10.1016/j.oceaneng.2024.118213>
- [16] Xu, M.T., Wang, L.Z., Wang, L.L., Guo, Z., Zhou, W.J. (2024). Influence of bounding surface plasticity-based soil-structure interaction model on integrated dynamic behaviour of jacket offshore wind turbines. *Ocean Engineering*, 298: 117204. <https://doi.org/10.1016/j.oceaneng.2024.117204>
- [17] Zhang, X.L., Zhang, B.J., Wang, D., Xu, C.S. (2024). Fatigue damage analysis method of offshore wind turbine foundation. *Ocean Engineering*, 302: 117618. <https://doi.org/10.1016/j.oceaneng.2024.117618>
- [18] Ngo, D.V., Kim, D.H. (2024). Seismic responses of different types of offshore wind turbine support structures. *Ocean Engineering*, 297: 117108. <https://doi.org/10.1016/j.oceaneng.2024.117108>
- [19] Dong, G.H., Guo, S.A., Bi, C.W. (2024). Numerical study on the flow characteristics of an integrated fish cage based on the monopile offshore wind turbine foundation. *Aquacultural Engineering*, 107: 102458. <https://doi.org/10.1016/j.aquaeng.2024.102458>
- [20] Li, J.L., Lian, J.J., Guo, Y.H., Wang, H.J. (2024). Concept design and floating installation method study of multi-bucket foundation floating platform for offshore wind turbines. *Marine Structures*, 93: 103541. <https://doi.org/10.1016/j.marstruc.2023.103541>
- [21] Ju, S.H., Mao, Y.C. (2024) Research on offshore wind turbine support structures under seismic soil liquefaction. *Ocean Engineering*, 304: 117750. <https://doi.org/10.1016/j.oceaneng.2024.117750>